

MonoLite3D: Lightweight 3D Object Properties Estimation

1st Ahmed El-Dawy
Electrical Power Department
Faculty of Engineering
Alexandria University
Alexandria, Egypt
ahmed.dawy@alexu.edu.eg

2nd Amr El-Zawawi
Electrical Power Department
Faculty of Engineering
Alexandria University
Alexandria, Egypt
amr.elzawawi@yahoo.com

3rd Mohamed El-Habrouk
Electrical Power Department
Faculty of Engineering
Alexandria University
Alexandria, Egypt
eepgmme1@yahoo.co.uk

Abstract—Reliable perception of the environment plays a crucial role in enabling efficient self-driving vehicles. Therefore, the perception system necessitates the acquisition of comprehensive 3D data regarding the surrounding objects within a specific time constrain, including their dimensions, spatial location and orientation. Deep learning has gained significant popularity in perception systems, enabling the conversion of image features captured by a camera into meaningful semantic information. This research paper introduces MonoLite3D network, an embedded-device friendly lightweight deep learning methodology designed for hardware environments with limited resources. MonoLite3D network is a cutting-edge technique that focuses on estimating multiple properties of 3D objects, encompassing their dimensions and spatial orientation, solely from monocular images. This approach is specifically designed to meet the requirements of resource-constrained environments, making it highly suitable for deployment on devices with limited computational capabilities. The experimental results validate the accuracy and efficiency of the proposed approach on the orientation benchmark of the KITTI dataset. It achieves an impressive score of 82.27% on the moderate class and 69.81% on the hard class, while still meeting the real-time requirements.

Index Terms—Computer vision, Perception, Deep learning, Autonomous driving, and Robotics

I. INTRODUCTION

Efficient 3D object properties estimation is a crucial research problem in various fields, including autonomous driving and robot grasping[1]. By accurately estimating the properties of 3D objects, the machines are enabled to interact with their environment more effectively and make informed decisions. In the context of autonomous driving, estimating the properties of 3D objects, such as their size, shape, and orientation, is essential for tasks like object detection, tracking, and motion planning[2]. This information helps autonomous vehicles understand the surrounding environment, predict object behavior, and make safe driving decisions[3].

The existing methods for detecting 3D objects can primarily be categorized as either relying on LIDAR-based methods or vision-based methods.[4]. LIDAR-based methods are precise and effective, but their high cost restricts their application in various industries[5]. There are two main types of vision-based methods[6]: monocular algorithms and binocular algorithms. Vision-based perception systems are commonly

utilized because they are affordable and offer a wide range of features. However, one major drawback of using monocular vision is that it cannot directly determine depth from image data. This limitation can lead to inaccuracies in estimating the three-dimensional pose of objects in monocular object detection. On the other hand, binocular vision, which provides more precise depth information compared to monocular vision, comes at a higher cost. Additionally, binocular vision has a narrower visual field range, which may not be suitable for certain operating conditions[7].

This study introduces MonoLite3D network, a lightweight technique based on deep learning that is designed to accurately determine the 3D characteristics of an object using the information obtained from a detected 2D bounding box. Cutting-edge 2D object detection models like YOLOv7[8], Detectron2[9], BERT[10] have the potential to evolve into 3D object detectors through the training of a compact and efficient feature extractor. This extractor would be responsible for capturing features from the input data, which can then be employed to predict both the orientation of the 3D bounding box of the object and its dimensions.

Section II of the paper discusses the existing research on the deep learning approaches used in 3D object detection. In Section III, the paper introduces MonoLite3D network and highlights its contributions, which are as follows:

- The simple design of MonoLite3D network which is composed of cheap operations.
- The choice of an efficient, lightweight, embedded device-friendly feature extractor alleviates the computational burden without sacrificing accuracy.

Section IV of the paper discusses the experimental work of the proposed MonoLite3D network. It provides information about the implementation details, the dataset used for training and benchmarking, and the training procedures. This section aims to provide a comprehensive understanding of how the MonoLite3D network was developed and evaluated. Experimental results on the KITTI benchmark confirm the effectiveness of the suggested MonoLite3D network architecture, as discussed in Section V. The paper concludes with a summary of findings in the final section.

II. RELATED WORK

This section offers a detailed overview of the current deep learning advancements in 3D object detection. It focuses on the different methods employed to generate 3D bounding boxes, as depicted in Figure 1.

A. 3D-Data Based Methods

In recent times, there has been notable progress in the field of 3D detection using LIDAR technology [11][12]. LIDAR sensors acquire precise 3D measurement data from their surroundings, represented as 3D points with absolute coordinates (x, y, z) . Given the inherent nature of LIDAR point cloud data, it is imperative to employ an architecture that enables efficient convolutional operations. Consequently, Deep Learning techniques employed for LIDAR-based 3D detection can be categorized into two main approaches: Point-based approaches and Voxel-based approaches [13][14].

Point-based Approaches: were developed to handle unprocessed and disorganized point clouds. Point-based techniques, including PointNet[15], utilize raw point clouds as input and extract point-level features for 3D object detection using structures like multi-layer perceptrons. Other models such as PointRCNN[16], RoarNet[17], and PointPainting[18] are instances of deep-learning neural networks that employ the Point-Based approach.

Voxel-Based Approaches: divide point clouds into equally sized 3D voxels. Then, for each voxel, features can be extracted from a group of points. This approach reduces the overall size of the point cloud and saves storage space[14]. Voxel-based techniques, such as VoxelNet[19], extend the 2D image representation to 3D space by dividing it into voxels. Other deep learning models, Center-based 3D object detection and tracking[20] and Afdet[21] utilize the Voxel-based approach for solving 3D object detection.

B. 2D-Data Based Methods

Deep-learning techniques that depend on 2D data primarily use RGB images as their main input. While 2D object detection networks have shown exceptional performance, the task of generating 3D bounding boxes solely from the 2D image plane is considerably more complex due to the absence of absolute depth information[22]. As a result, approaches for 3D object detection using 2D data can be categorized based on how they address the challenge of obtaining depth information. These categories include Depth-Aided Based Approaches, Stereo-Graphically Based Approaches, and Single Image Based Approaches.

Depth-Aided Based Approaches: As a result of the absence of depth information in single monocular images, several studies have attempted to leverage advancements in depth estimation neural networks. In earlier studies [23][24], images are transformed into pseudo-LIDAR representations by utilizing readily available depth map predictors and calibration parameters. Subsequently, established LIDAR-based 3D detection methods are applied to generate 3D bounding

boxes, albeit with reduced effectiveness. In contrast, DDMP-3D [25] emphasize a fusion-based approach that cleverly integrates information from both images and estimated depth through specially designed deep convolutional neural networks (CNNs). However, most of the previously mentioned methods that directly rely on off-the-shelf depth estimators incur significant computational overhead and yield only marginal improvements due to the inherent inaccuracies in the estimated depth maps[26].

Stereo-Graphically Based Approaches: Approaches outlined in [27][28][29] involve the processing of a pair of stereo images using a Siamese network. These methods then generate a 3D cost volume, which is utilized to determine the matching cost for stereo matching through neural networks. Additionally, MVS-Machine[30] adopts a differentiable approach involving projection and re-projection to enhance the construction of a 3D volume from multi-view images.

Single Image Based Approaches: In recent studies [31][32], the focus has shifted towards using only a single monocular RGB image as input for 3D object detection. For instance, PGD-FCOS3D[33] introduces geometric correlation graphs among detected objects and leverages these constructed graphs to enhance depth estimation accuracy. Other approaches such as RTM3D[34] and SMOKE[35] anticipate key points of the 3D bounding box as a complementary step to establish spatial information about observed objects. MonoCInIS[36] proposes a method that utilizes instance segmentation to estimate an object's pose, and it is designed to be camera-independent to account for different camera perspectives. Many recent studies build upon a prior 2D object detection stage. For example, Deep3Dbox[37] presents an innovative approach for predicting object orientation and dimensions. M3D-RPN[38] incorporates depth-aware convolution to anticipate 3D objects and generate 3D object properties while satisfying 2D detection requirements. Consequently, PoseCNN[39] identifies an object's position in a 2D image while simultaneously predicting its depth to determine its 3D position. It's worth noting that estimating 3D rotation directly with PoseCNN is challenging because the rotation space is nonlinear, as pointed out in[7].

III. MONOLITE3D NETWORK

By making the assumption that the perspective projection of a 3D bounding box should closely align with its 2D detection window, it becomes feasible to leverage the achievements of previous research in the field of 2D object detection for the estimation of 3D bounding boxes, as demonstrated in earlier work such as[40]. The 3D bounding box can be defined by its dimensional attributes $D = [d_x, d_y, d_z]$, central coordinates $T = [t_x, t_y, t_z]^T$, and orientation $R(\theta, \phi, \alpha)$, where these parameters are defined by azimuth (θ), elevation (ϕ), and roll (α) angles. In scenarios where the ground is assumed to be flat, it is safe to assume that ϕ and α angles are both zero. Furthermore, when all objects are considered to be on the ground, it is reasonable to set the object's height (t_y) to zero. Subsequently, The projection of a 3D point from the object's

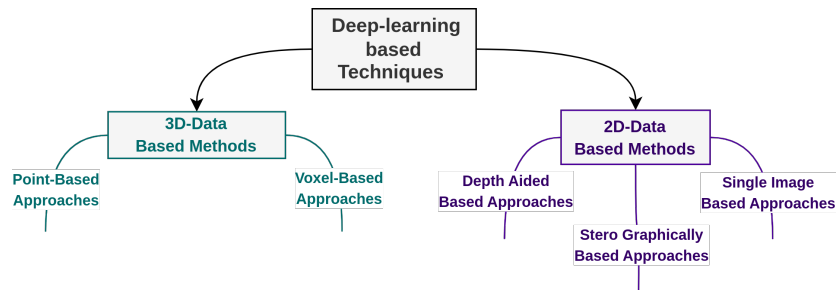


Fig. 1. 3D object detection deep learning methodologies.

coordinate frame, denoted as $X_o = [X, Y, Z, 1]^T$, to the image frame, represented as $x = [u, v, 1]^T$, is given by the following equation as detailed in[37],[41],[42]:

$$x = K \begin{bmatrix} R & T \end{bmatrix} X_o \quad (1)$$

This transformation is performed based on the object's pose within the camera coordinate frame $(R, T) \in SE(3)$ and the intrinsic matrix of the camera, denoted as K .

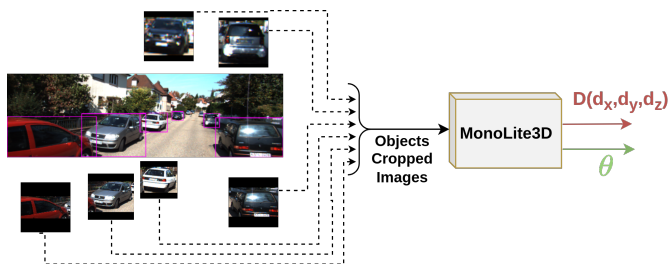


Fig. 2. The general architecture of the proposed MonoLite3D network is composed of one stage, which is the Orientation-Dimensions Estimator stage.

While projecting a 3D point from the object's coordinate frame onto the image plane is straightforward, it results in the loss of depth information. Conversely, projecting a point from the image back into the 3D object's coordinate frame is a complex task. To recover 3D object coordinates from a 2D image, comprehensive feature estimation is vital. That's why the MonoLite3D network prioritizes object orientation and dimensions. Consequently, MonoLite3D network is composed of one main stage as presented in Figure 2 :

- The Orientation-Dimensions Estimator stage takes the cropped object image as input, proceeds to extract visual characteristics of the object, and subsequently generates the object's geometric attributes, including orientation and dimensions.

A. Orientation Estimation

Estimating the object's overall orientation, denoted as $R \in SO(3)$, requires more than just the 2D bounding box information. It also depends on the box's position in the image plane. For instance, consider the rotation $R(\theta)$, where θ (yaw) represents azimuth, as shown in Figure 3. Consider the example of a vehicle moving in a straight line. Here,

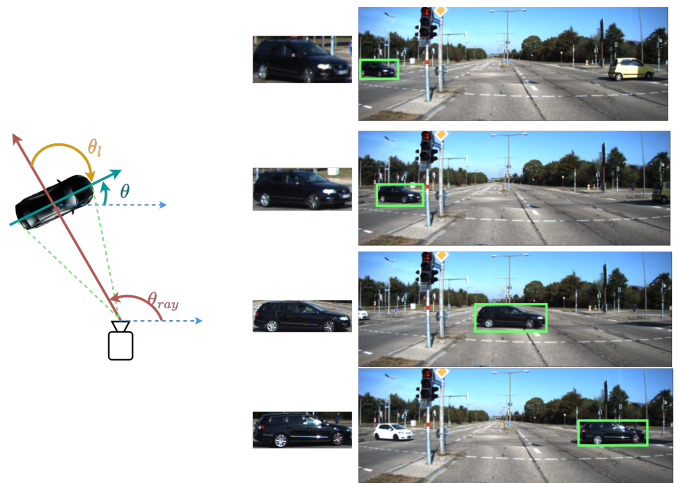


Fig. 3. The object's orientation, denoted as θ , is computed by adding θ_{ray} and θ_l together. The Orientation-Dimensions Estimator provides the value for θ_l , while θ_{ray} can be determined in relation to the center of the object's bounding box using the known camera intrinsic parameters.

the global orientation $R(\theta)$ remains constant, but the local orientation θ_l based on the vehicle's appearance within the 2D bounding box, changes. Determining the overall direction $R(\theta)$ involves combining the variation in the local direction θ_l relative to the ray passing through the bounding box's center. This process is aided by computing the ray's direction at a specific pixel using intrinsic camera parameters θ_{ray} . To summarize, the steps include predicting local orientation from 2D bounding box features (θ_l), then combining this with the ray's direction (θ_{ray}) toward the bounding box's center to calculate the object's global orientation.

Object detectors like Yolo and SSD[43] employ anchor boxes to define potential bounding box modes and compute adjustments for each anchor box. Similarly, MultiBin architecture[37] adopts a related concept for orientation estimation. It discretizes the angle space into overlapping bins, where each bin is associated with score probabilities ($score_i$) for the angle falling within it and residual correction angles to align with the center ray of the bin. These corrections are represented by sine and cosine values, yielding three outputs per bin ($score_i, sine(\Delta\theta_i), cosine(\Delta\theta_i)$).

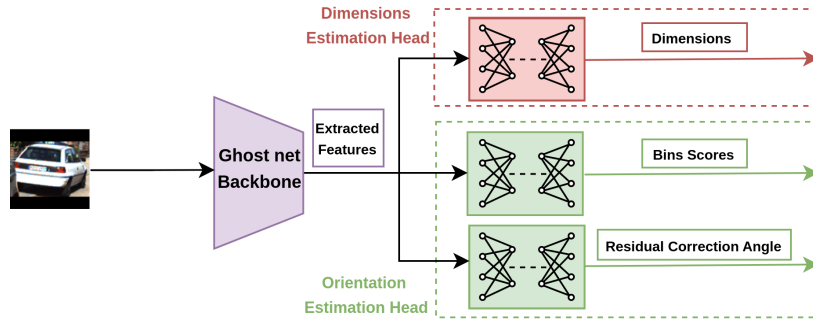


Fig. 4. Orientation-Dimensions Estimation heads.

Consequently, the total loss for the MultiBin orientation is:

$$L_{\theta} = L_{score} + \alpha \times L_{residual} \quad (2)$$

The softmax loss [44] computes the score loss L_{score} for each bin. The residual loss $L_{residual}$ minimizes the difference between the estimated angle and the ground truth angle within the relevant bin. Thus, $L_{residual}$ maximizes cosine distance and is calculated as:

$$L_{residual} = \frac{1}{n_{\theta^*}} \sum \cos(\theta^* - c_i - \Delta\theta_i) \quad (3)$$

where n_{θ^*} is the number of bins spanning the ground truth angle θ^* . c_i is the angle of the bin's i centre. $\Delta\theta_i$ is the adjustment that must be made to the centre of the bin i .

As depicted in Figure 4, the Orientation-Dimensions estimator employs Ghostnet [45] as its backbone for extracting meaningful visual object features. Subsequently, these extracted features are shared across three distinct fully connected branches. The first branch consists of (1280, 256, 3) fully connected units and is responsible for estimating object dimensions. In contrast, the second branch comprises (1280, 256, 2) fully connected units to produce bin scores. Lastly, the third branch is composed of (1280, 256, 2x2) fully connected units, generating residual correction angles in both sine and cosine representations.

B. Dimensions Estimation

The KITTI dataset[46] includes distinct categories such as cars, vans, trucks, pedestrians, cyclists, and buses, each of which exhibits noticeable similarities in terms of shape and size among objects. For each dimension, it is convenient to predict the deviation value from the mean parameter value computed across the training dataset. The loss for dimension estimation can be computed as follows [37]:

$$L_{Dimensions} = \frac{1}{n} \sum (D^* - \bar{D} - \delta)^2 \quad (4)$$

Here, D^* represents the true dimensions of 3D bounding boxes, \bar{D} denotes the mean dimensions of objects within a specific class, n stands for the number of objects in the training batch, and δ represents the predicted deviation value relative to the average value predicted by the neural network.

C. GhostNet As An Off The shelf Lightweight Feature Extractor

Feature maps are spatial representations derived from applying convolution layers to input data. These maps capture specific image characteristics based on learned filter weights. Within standard convolution layers, it's observed that numerous similar intrinsic features exist across all feature maps, termed "Ghost Feature Maps" [45]. GhostNet's core aim is to reduce parameters and FLOPs while maintaining performance close to the original feature maps. It accomplishes this by generating some output feature maps and using a low-cost linear operation for the rest, resulting in fewer parameters and FLOPs. This operation adapts to input data and supports optimization through backpropagation [45]. GhostNet's effectiveness as a feature extractor is evident in various applications [47], [48], [49], particularly in tasks like the Orientation-Dimensions Estimator. This efficient design allows the MonoLite3D network to have a combined parameter count of only 5.61 million while preserving estimation accuracy.

IV. EXPERIMENTAL WORK

A. Implementation Details

As discussed earlier, the proposed MonoLite3D network extracts an object's 3D properties from a monocular image's 2D bounding box. This is achieved through a key stage, depicted in Figure 4, which includes a feature extractor and three interconnected branches sharing extracted features. Its main function is to estimate the object's 3D dimensions and orientation.

B. Dataset

The KITTI dataset, introduced in [46], provides a widely accessible open-source resource for evaluating learning-based approaches in realistic autonomous driving scenarios. Performance evaluation is categorized based on factors like occlusion, truncation level, and the visible height of object instances' 2D bounding boxes, resulting in easy, moderate, and hard test cases as detailed in [46]. The dataset also includes benchmarks like 2D Object Detection and Orientation, used to evaluate the MonoLite3D network's orientation estimation performance.

1) *Data Augmentation*: To enhance the training dataset, enhance the training procedure, and mitigate overfitting, various data augmentation methods were applied. These techniques encompass the introduction of random Gaussian noise, optical distortion (with a 0.5 probability), and random fog (with an 0.8 probability).



Fig. 5. The general architecture of the proposed MonoLite3D network is composed of one stage, which is the Orientation-Dimensions Estimator stage.

2) *Preprocessing*: Complex preprocessing techniques were deliberately avoided when handling the dataset. Instead, the sole preprocessing operation involved applying resizing with padding to the cropped 2D image of the detected object. This step’s purpose is to retain the object’s inherent characteristics before passing it on to either the Orientation-Dimensions Estimator or the Bird’s Eye View Center Estimator. This approach ensures that object properties are preserved, rather than risking the loss of these properties through scaling alone, as depicted in Figure 5.

C. Training

The training of the MonoGhost network was conducted using a Geforce RTX 3060 Ti 8G graphics card. The choice of optimizer for this process was AdamW, as detailed in [50], with a weight decay parameter of $1e-3$.

1) *Orientation-Dimensions Estimator*: The Orientation-Dimensions Estimator was trained with a batch size of 200 for a total of 250 epochs. Initially, the learning rate was set to $1e-4$. The training employed a scheduler configured to reduce the learning rate on a plateau, with a reduction factor of 0.1, a patience of 10 epochs, and a threshold of $1e-4$. The chosen optimizer for this task was AdamW, incorporating a weight decay of $1e-3$.

V. RESULTS AND DISCUSSIONS

Given that the MonoLite3D network, as presented, consists of a single primary stage, its performance can be evaluated using the KITTI object orientation benchmark. To facilitate this benchmark, an off-the-shelf 2D object detector was employed, Faster RCNN[51], to provide the coordinates of the 2D bounding boxes.

TABLE I shows the proposed MonoLite3D network results for orientation on KITTI benchmark.

The MonoLite3D network’s main contributions are its efficient design, based on lightweight operations, and the

TABLE I
MONOLITE3D NETWORK ORIENTATION SCORE ON KITTI BENCHMARK.

Benchmark	Easy	Moderate	Hard
Car (Detection)	90.79 %	83.33 %	71.13 %
Car (Orientation)	90.23 %	82.27 %	69.81 %

TABLE II
COMPARISON OF MONOLITE3D NETWORK ORIENTATION SCORES ON THE “CAR” CLASS WITHIN THE KITTI BENCHMARK, ACROSS DIFFERENT DIFFICULTY LEVELS: EASY, MODERATE, AND HARD. THE TABLE PRESENTS MONOLITE3D’S ORIENTATION PERFORMANCE ALONGSIDE OTHER STATE-OF-THE-ART MODELS, HIGHLIGHTING ITS EFFECTIVENESS IN ESTIMATING ORIENTATION FOR CAR OBJECTS.

Model	Easy	Moderate	Hard	Inference Time
CMAN[52]	89.43 %	81.96 %	63.74 %	0.15 s
D4LCN[53]	90.01 %	82.08 %	63.98 %	0.2 s
Pseudo-LiDAR++[54]	94.14 %	81.87 %	74.29 %	0.4 s
Disp R-CNN[55]	93.49 %	81.96 %	67.35 %	0.387 s
MonoLite3D	90.23 %	82.27 %	69.81 %	0.01514 s

use of a lightweight feature extractor. Evaluating its real-time performance is essential. On a Geforce RTX 3060 Ti 8G, it achieves an average inference time of 0.0121 seconds for a batch of 200 objects, while on a GeForce GTX 1050 Ti, it averages 0.01514 seconds. These results confirm its real-time capability, even on less powerful GPUs. MonoLite3D network highlights that using the MultiBin discrete-continuous approach for orientation estimation, in combination with a lightweight feature extractor, significantly improves performance.

The remarkable performance of MonoLite3D extends beyond its accuracy, showcasing efficiency on limited hardware resources. As illustrated in TABLE II, across difficulty levels on the KITTI benchmark, particularly in Moderate (82.27%) and Hard (69.81%) cases, MonoLite3D outperforms competing models, including CMAN[52], D4LCN[53], Pseudo-LiDAR++[54], and Disp R-CNN. Notably[55], MonoLite3D achieves these commendable orientation scores within an impressive execution time of just 0.01514 seconds on the cost-effective GeForce GTX 1050 Ti, significantly outpacing the inference times of other models such as CMAN[52] (0.15 s), D4LCN[53] (0.2 s), Pseudo-LiDAR++[54] (0.4 s), and Disp R-CNN[55]. Notably (0.387 s). This not only positions MonoLite3D as a leader in accuracy but also underscores its unparalleled real-time capabilities. The model’s superior performance on both accuracy and efficiency fronts makes it an efficient and practical choice for real-world applications, ensuring precise orientation estimation while operating on resource-constrained hardware.

VI. CONCLUSION

This paper introduced an innovative and lightweight architectural solution for the estimation of complete 3D geometric characteristics of known object classes from a single

image. The MonoLite3D network, designed for monocular 3D geometric feature estimation, demonstrates promising levels of accuracy. It achieves results of 90.23%, 82.27%, and 69.81% on the KITTI object orientation benchmark, all while maintaining an average inference time of just 0.033 seconds per batch of 70 objects. This proposed network exhibits the potential for seamless integration with state-of-the-art 2D object detection platforms, making it a viable choice for deployment in autonomous vehicles and robotic navigation systems.

REFERENCES

- [1] Y. Liu, Y. Yixuan, and M. Liu, "Ground-aware monocular 3d object detection for autonomous driving," *IEEE Robotics and Automation Letters*, vol. 6, no. 2, pp. 919–926, 2021.
- [2] S. Calvert, W. Schakel, and J. Van Lint, "Will automated vehicles negatively impact traffic flow?" *Journal of advanced transportation*, vol. 2017, 2017.
- [3] D. Sharma, "Evaluation and analysis of perception systems for autonomous driving," 2020.
- [4] Z. Li, Y. Du, M. Zhu, S. Zhou, and L. Zhang, "A survey of 3d object detection algorithms for intelligent vehicles development," *Artificial Life and Robotics*, pp. 1–8, 2022.
- [5] Y. Wu, Y. Wang, S. Zhang, and H. Ogai, "Deep 3d object detection networks using lidar data: A review," *IEEE Sensors Journal*, vol. 21, no. 2, pp. 1152–1171, 2020.
- [6] R. Qian, X. Lai, and X. Li, "3d object detection for autonomous driving: a survey," *Pattern Recognition*, vol. 130, p. 108796, 2022.
- [7] J. Wu, D. Yin, J. Chen, Y. Wu, H. Si, and K. Lin, "A survey on monocular 3d object detection algorithms based on deep learning," in *Journal of Physics: Conference Series*, vol. 1518, no. 1. IOP Publishing, 2020, p. 012049.
- [8] C.-Y. Wang, A. Bochkovskiy, and H.-Y. M. Liao, "Yolov7: Trainable bag-of-freebies sets new state-of-the-art for real-time object detectors," *arXiv preprint arXiv:2207.02696*, 2022.
- [9] A. V. S. Abhishek and S. Kotni, "Detectron2 object detection & manipulating images using cartoonization," *Int. J. Eng. Res. Technol.(IJERT)*, vol. 10, 2021.
- [10] C. Resnick, O. Litany, A. Kar, K. Kreis, J. Lucas, K. Cho, and S. Fidler, "Causal scene bert: Improving object detection by searching for challenging groups of data," *arXiv preprint arXiv:2202.03651*, 2022.
- [11] J. Li, Y. Sun, S. Luo, Z. Zhu, H. Dai, A. S. Krylov, Y. Ding, and L. Shao, "P2v-renn: point to voxel feature learning for 3d object detection from point clouds," *IEEE Access*, vol. 9, pp. 98 249–98 260, 2021.
- [12] J. Li, S. Luo, Z. Zhu, H. Dai, A. S. Krylov, Y. Ding, and L. Shao, "3d iou-net: Iou guided 3d object detector for point clouds," *arXiv preprint arXiv:2004.04962*, 2020.
- [13] J. Mao, S. Shi, X. Wang, and H. Li, "3d object detection for autonomous driving: a review and new outlooks," *arXiv preprint arXiv:2206.09474*, 2022.
- [14] D. Fernandes, A. Silva, R. Névoa, C. Simões, D. Gonzalez, M. Guevara, P. Novais, J. Monteiro, and P. Melo-Pinto, "Point-cloud based 3d object detection and classification methods for self-driving applications: A survey and taxonomy," *Information Fusion*, vol. 68, pp. 161–191, 2021. [Online]. Available: <https://www.sciencedirect.com/science/article/pii/S1566253520304097>
- [15] C. R. Qi, H. Su, K. Mo, and L. J. Guibas, "Pointnet: Deep learning on point sets for 3d classification and segmentation," in *Proceedings of the IEEE conference on computer vision and pattern recognition*, 2017, pp. 652–660.
- [16] S. Shi, X. Wang, and H. Li, "Pointcn: 3d object proposal generation and detection from point cloud," in *Proceedings of the IEEE/CVF conference on computer vision and pattern recognition*, 2019, pp. 770–779.
- [17] K. Shin, Y. P. Kwon, and M. Tomizuka, "Roarnet: A robust 3d object detection based on region approximation refinement," in *2019 IEEE intelligent vehicles symposium (IV)*. IEEE, 2019, pp. 2510–2515.
- [18] S. Vora, A. H. Lang, B. Helou, and O. Beijbom, "Pointpainting: Sequential fusion for 3d object detection," in *Proceedings of the IEEE/CVF conference on computer vision and pattern recognition*, 2020, pp. 4604–4612.
- [19] Y. Zhou and O. Tuzel, "Voxelnet: End-to-end learning for point cloud based 3d object detection," in *Proceedings of the IEEE conference on computer vision and pattern recognition*, 2018, pp. 4490–4499.
- [20] T. Yin, X. Zhou, and P. Krahenbuhl, "Center-based 3d object detection and tracking," in *Proceedings of the IEEE/CVF conference on computer vision and pattern recognition*, 2021, pp. 11 784–11 793.
- [21] R. Ge, Z. Ding, Y. Hu, Y. Wang, S. Chen, L. Huang, and Y. Li, "Afdet: Anchor free one stage 3d object detection," *arXiv preprint arXiv:2006.12671*, 2020.
- [22] M. M. Rahman, Y. Tan, J. Xue, and K. Lu, "Notice of violation of IEEE publication principles: Recent advances in 3d object detection in the era of deep neural networks: A survey," *IEEE Transactions on image processing*, vol. 29, pp. 2947–2962, 2019.
- [23] X. Ma, Z. Wang, H. Li, P. Zhang, W. Ouyang, and X. Fan, "Accurate monocular 3d object detection via color-embedded 3d reconstruction for autonomous driving," in *Proceedings of the IEEE/CVF International Conference on Computer Vision*, 2019, pp. 6851–6860.
- [24] Y. Wang, W.-L. Chao, D. Garg, B. Hariharan, M. Campbell, and K. Q. Weinberger, "Pseudo-lidar from visual depth estimation: Bridging the gap in 3d object detection for autonomous driving," in *Proceedings of the IEEE/CVF Conference on Computer Vision and Pattern Recognition*, 2019, pp. 8445–8453.
- [25] L. Wang, L. Du, X. Ye, Y. Fu, G. Guo, X. Xue, J. Feng, and L. Zhang, "Depth-conditioned dynamic message propagation for monocular 3d object detection," in *Proceedings of the IEEE/CVF Conference on Computer Vision and Pattern Recognition*, 2021, pp. 454–463.
- [26] K.-C. Huang, T.-H. Wu, H.-T. Su, and W. H. Hsu, "Monodtr: Monocular 3d object detection with depth-aware transformer," in *Proceedings of the IEEE/CVF Conference on Computer Vision and Pattern Recognition*, 2022, pp. 4012–4021.
- [27] Y. Wang, Z. Lai, G. Huang, B. H. Wang, L. Van Der Maaten, M. Campbell, and K. Q. Weinberger, "Anytime stereo image depth estimation on mobile devices," in *2019 international conference on robotics and automation (ICRA)*. IEEE, 2019, pp. 5893–5900.
- [28] A. Kendall, H. Martirosyan, S. Dasgupta, P. Henry, R. Kennedy, A. Bachrach, and A. Bry, "End-to-end learning of geometry and context for deep stereo regression," in *Proceedings of the IEEE international conference on computer vision*, 2017, pp. 66–75.
- [29] F. Zhang, V. Prisacariu, R. Yang, and P. H. Torr, "Ga-net: Guided aggregation net for end-to-end stereo matching," in *Proceedings of the IEEE/CVF Conference on Computer Vision and Pattern Recognition*, 2019, pp. 185–194.
- [30] A. Kar, C. Häne, and J. Malik, "Learning a multi-view stereo machine," *Advances in neural information processing systems*, vol. 30, 2017.
- [31] A. Simonelli, S. R. Bulò, L. Porzi, E. Ricci, and P. Kotschieder, "Towards generalization across depth for monocular 3d object detection," in *Computer Vision—ECCV 2020: 16th European Conference, Glasgow, UK, August 23–28, 2020, Proceedings, Part XXII 16*. Springer, 2020, pp. 767–782.
- [32] Y. Zhang, J. Lu, and J. Zhou, "Objects are different: Flexible monocular 3d object detection," in *Proceedings of the IEEE/CVF Conference on Computer Vision and Pattern Recognition*, 2021, pp. 3289–3298.
- [33] T. Wang, X. Zhu, J. Pang, and D. Lin, "Probabilistic and geometric depth: Detecting objects in perspective," in *Conference on Robot Learning (CoRL)*, 2021.
- [34] P. Li, H. Zhao, P. Liu, and F. Cao, "Rtm3d: Real-time monocular 3d detection from object keypoints for autonomous driving," in *Computer Vision—ECCV 2020: 16th European Conference, Glasgow, UK, August 23–28, 2020, Proceedings, Part III 16*. Springer, 2020, pp. 644–660.
- [35] Z. Liu, Z. Wu, and R. Tóth, "Smoke: Single-stage monocular 3d object detection via keypoint estimation," in *Proceedings of the IEEE/CVF Conference on Computer Vision and Pattern Recognition Workshops*, 2020, pp. 996–997.
- [36] J. Heylen, M. De Wolf, B. Dawagne, M. Proesmans, L. Van Gool, W. Abbeloos, H. Abdelkawy, and D. O. Reino, "Monocinis: Camera independent monocular 3d object detection using instance segmentation," in *Proceedings of the IEEE/CVF International Conference on Computer Vision*, 2021, pp. 923–934.
- [37] A. Mousavian, D. Anguelov, J. Flynn, and J. Kosecka, "3d bounding box estimation using deep learning and geometry," in *Proceedings of the IEEE conference on Computer Vision and Pattern Recognition*, 2017, pp. 7074–7082.

- [38] G. Brazil and X. Liu, "M3d-rpn: Monocular 3d region proposal network for object detection," in *Proceedings of the IEEE/CVF International Conference on Computer Vision*, 2019, pp. 9287–9296.
- [39] Y. Xiang, T. Schmidt, V. Narayanan, and D. Fox, "Posecnn: A convolutional neural network for 6d object pose estimation in cluttered scenes," *arXiv preprint arXiv:1711.00199*, 2017.
- [40] S. Huang, Y. Chen, T. Yuan, S. Qi, Y. Zhu, and S.-C. Zhu, "Perspectivenet: 3d object detection from a single rgb image via perspective points," *Advances in neural information processing systems*, vol. 32, 2019.
- [41] K. Daniilidis and R. Klette, *Imaging beyond the pinhole camera*. Springer, 2006.
- [42] F. Gu, H. Zhao, Y. Ma, and P. Bu, "Camera calibration based on the back projection process," *Measurement Science and Technology*, vol. 26, no. 12, p. 125004, 2015.
- [43] W. Liu, D. Anguelov, D. Erhan, C. Szegedy, S. Reed, C.-Y. Fu, and A. C. Berg, "Ssd: Single shot multibox detector," in *Computer Vision—ECCV 2016: 14th European Conference, Amsterdam, The Netherlands, October 11–14, 2016, Proceedings, Part I 14*. Springer, 2016, pp. 21–37.
- [44] B. Kingsbury, "Lattice-based optimization of sequence classification criteria for neural-network acoustic modeling," in *2009 IEEE International Conference on Acoustics, Speech and Signal Processing*. IEEE, 2009, pp. 3761–3764.
- [45] K. Han, Y. Wang, Q. Tian, J. Guo, C. Xu, and C. Xu, "Ghostnet: More features from cheap operations," in *Proceedings of the IEEE/CVF conference on computer vision and pattern recognition*, 2020, pp. 1580–1589.
- [46] A. Geiger, P. Lenz, and R. Urtasun, "Are we ready for autonomous driving? the kitti vision benchmark suite," in *2012 IEEE conference on computer vision and pattern recognition*. IEEE, 2012, pp. 3354–3361.
- [47] L. Ting, Z. Baijun, Z. Yongsheng, and Y. Shun, "Ship detection algorithm based on improved yolo v5," in *2021 6th International Conference on Automation, Control and Robotics Engineering (CACRE)*. IEEE, 2021, pp. 483–487.
- [48] D. Zhou, B. Wang, C. Zhu, F. Zhou, and H. Wu, "A light-weight feature extractor for lithium-ion battery health prognosis," *Reliability Engineering & System Safety*, p. 109352, 2023.
- [49] J. Chi, S. Guo, H. Zhang, and Y. Shan, "L-ghostnet: Extract better quality features," *IEEE Access*, vol. 11, pp. 2361–2374, 2023.
- [50] I. Loshchilov and F. Hutter, "Decoupled weight decay regularization," *arXiv preprint arXiv:1711.05101*, 2017.
- [51] R. Girshick, "Fast r-cnn," in *Proceedings of the IEEE international conference on computer vision*, 2015, pp. 1440–1448.
- [52] Y. L. C. R. C. L. Yuanzhouhan Cao, Hui Zhang, "Cman: Learning global structure correlation for monocular 3d object detection," *IEEE Trans. Intell. Transport. Syst.*, 2022.
- [53] M. Ding, Y. Huo, H. Yi, Z. Wang, J. Shi, Z. Lu, and P. Luo, "Learning depth-guided convolutions for monocular 3d object detection," in *Proceedings of the IEEE/CVF Conference on computer vision and pattern recognition workshops*, 2020, pp. 1000–1001.
- [54] Y. You, Y. Wang, W.-L. Chao, D. Garg, G. Pleiss, B. Hariharan, M. Campbell, and K. Q. Weinberger, "Pseudo-lidar++: Accurate depth for 3d object detection in autonomous driving," in *ICLR*, 2020.
- [55] J. Sun, L. Chen, Y. Xie, S. Zhang, Q. Jiang, X. Zhou, and H. Bao, "Disp r-cnn: Stereo 3d object detection via shape prior guided instance disparity estimation," in *CVPR*, 2020.